

# The missing aerosol response in twentieth-century mid-latitude precipitation observations

Joe M. Osborne<sup>\*</sup> and F. Hugo Lambert

**Regional temperature change over the twentieth century has been strongly influenced by aerosol forcing<sup>1,2</sup>. The aerosol effect is also expected to be pronounced on regional precipitation change<sup>3</sup>. Changes in historical precipitation—for the global mean and land mean of certain regions—should be more sensitive to spatially heterogeneous aerosol forcing than greenhouse gas forcing<sup>4–7</sup>. Here, we investigate whether regional precipitation and temperature respond predictably to a significant strengthening in mid-twentieth-century Northern Hemisphere mid-latitude (NHML) aerosol forcing. Using the latest climate model experiments, we find that observed regional temperature changes and observed Northern Hemisphere tropical land precipitation changes are consistent with the IPCC Fifth Assessment Report<sup>8</sup> aerosol forcing estimate, but observed NHML land precipitation changes show little evidence of an aerosol response. This may be a result of changes in precipitation measurement practice that increased observed precipitation totals at the same time that aerosol forcing was expected to reduce them<sup>9</sup>. Investigating this inconsistency, we calculate the required increase in early-twentieth-century observed NHML land precipitation to bring this result in line with aerosol forcing. Biases greater than this calculated correction have been identified in countries within the NHML region previously, notably the former Soviet Union<sup>9,10</sup>. These observations are frequently used as a metric for the quality of model-simulated precipitation. More homogeneity studies would be of huge benefit.**

Twentieth-century climate change has been dominated by greenhouse gas (GHG)-driven warming<sup>11</sup>, interrupted by a mid-twentieth-century period of slight cooling probably driven by aerosols, both globally and in the Northern Hemisphere mid-latitude (NHML) region. The NHML land region has been the source for a large proportion of global emissions originating from human activity<sup>12</sup>, including short-lived forcing agents such as aerosols. Our longest, most comprehensive temperature and precipitation observations also exist here. These have allowed for the identification of a temperature response to aerosol forcing in observations and climate models<sup>1</sup>. However, no such link between precipitation and local aerosol forcing in the NHML land region has been reported. Here, we consider whether one should be expected and if it is found in observations and models.

In the global mean, energetic constraints dictate that precipitation change is more sensitive to aerosol forcing than GHG forcing per unit temperature change<sup>4,5</sup>. The direct effect of GHG forcing counteracts surface temperature-dependent precipitation change, whereas the direct effect of sulphate aerosol forcing is negligible<sup>13,14</sup>. Figure 1a shows the five-year global mean precipitation–temperature relationship for three

twentieth-century experiments driven with different forcings using the CanESM2 climate model. Both the experiment forced only by GHGs and the anthropogenic aerosol alone experiment have a linear precipitation–temperature relationship, but the change in precipitation per unit change in temperature is greater in the latter. The all-forcings experiment reflects the temporal evolution of twentieth-century GHG and anthropogenic aerosol forcing. As GHG forcing and temperature increase in proportion in the early twentieth century, precipitation also increases. Aerosol concentrations increase markedly in the mid twentieth century<sup>12</sup>, initiating a slight temperature decrease and a larger decrease in precipitation. Precipitation at the end of the twentieth century increases in line with GHG-driven warming. Hence, the twentieth-century precipitation–temperature relationship looks like two GHG-driven straight lines ‘offset’ by mid-twentieth-century aerosol-driven cooling (Methods).

Mid-twentieth-century aerosol emissions induced an interhemispheric forcing asymmetry that has been accredited with the southward shift of the tropical rain belt seen in models and observations<sup>6,7</sup>, drying the Northern Hemisphere tropical (NHT) region and wetting the Southern Hemisphere tropics. Therefore, the five-year NHT land mean precipitation–global mean temperature relationship (Fig. 1b) is comparable to that in Fig. 1a in all three experiments, demonstrating a precipitation response to largely remote NHML aerosol forcing. However, aerosol forcing is also expected to decrease the local hydrological cycle in most situations, by cooling the surface and encouraging local atmospheric subsidence (sulphate) or through increasing atmospheric radiative absorption (black carbon). Indeed, idealized experiments have demonstrated that local aerosol forcing can cause large circulation changes and an associated reduction in NHML precipitation<sup>3</sup>. Modelled NHML land mean precipitation shares a similar relationship with global mean temperature as both global mean precipitation and NHT land mean precipitation (Fig. 1c), so we expect to see evidence for an aerosol response in NHML land precipitation observations.

Figure 2a shows the surface temperature gradient anomalies from the HadCRUT4 data set<sup>15</sup> and output from historically forced runs of 23 climate models (Supplementary Table 1) participating in the Coupled Model Intercomparison Project Phase 5 (CMIP5). Here, mean temperature gradient (land and ocean) is defined as the difference between NHML surface temperature anomalies and Southern Hemisphere extratropical (SHEXT) surface temperature anomalies (Methods). Temperature anomalies in the SHEXT region show continual warming in the absence of significant local aerosol forcing; thus, the gradient change accentuates the temperature response to aerosols in the NHML region. The observations and most models show a mid-twentieth-century hiatus or downward

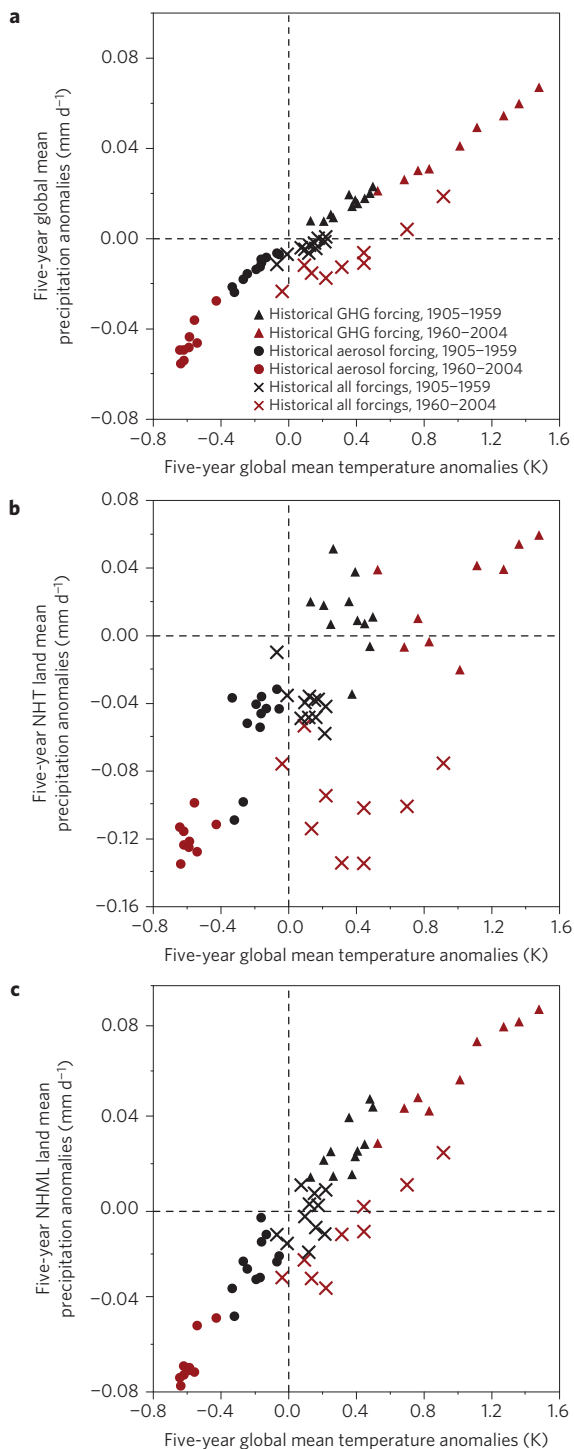


**Figure 1 | Five-year precipitation–temperature relationships for three twentieth-century experiments with CanESM2 for 1905–2004.**

**a**, Five-year global mean precipitation–temperature relationships. **b**, Five-year NHT land mean precipitation–global mean temperature relationships. **c**, Five-year Northern Hemisphere mid-latitude land mean precipitation–global mean temperature relationships. Three twentieth-century experiments are included—one driven by greenhouse gas (GHG) forcings alone, one driven by anthropogenic aerosol forcings alone and one driven by all forcings. Five members contribute towards the ensemble mean of each experiment, with anomalies given relative to the mean of a pre-industrial control simulation. Temperature is masked to HadCRUT4 observations (Methods). Precipitation in **b** and **c** is masked to Global Historical Climatology Network observations (Methods).

trend, but the models do not simulate the observed abrupt decrease in the late 1960s (ref. 16), which is widely attributed to internal variability<sup>17</sup>. Significant warming again dominates in the late twentieth century. Most models and Global Historical Climatology Network (GHCN) data set<sup>18</sup> precipitation observations show a NHT land mean mid-twentieth-century drying, followed by a late-twentieth-century wetting (Fig. 2b). This telltale aerosol signature is also evident when considering all Northern Hemisphere land masses<sup>19,20</sup>, with the NHT land region driving the trends (Supplementary Fig. 1). There is no overall twentieth-century trend in model simulated NHML land mean precipitation anomalies (Fig. 2c), consistent with simulated NHT land mean precipitation anomalies and simulated global mean precipitation anomalies (Supplementary Fig. 2). However, there is a positive trend in observed NHML land mean precipitation anomalies, with no evidence of a mid-twentieth-century drying signal. We check for consistency with three other gridded observational precipitation data sets (Methods). All four data sets show a near-identical positive trend (Supplementary Fig. 3) and no evidence for an aerosol-driven drying.

Changes in mean temperature gradient, NHT land mean precipitation and NHML land mean precipitation are seemingly more sensitive to spatially heterogeneous (mostly NHML) aerosol forcing than more homogeneous GHG forcing. We now test the extent to which the varying strength of NHML surface aerosol forcing (Methods), in models and the real world, manifests itself in the magnitude of the departure, or offset, from an otherwise linear GHG-driven response. For all 23 models and the observations, the size of the mid-twentieth-century offset is measured by fitting a simple linear regression model (Methods) to the relationship of each variable with global mean temperature in turn. The temperature gradient (Fig. 3a), NHT land precipitation (Fig. 3b) and NHML land precipitation (Fig. 3c) offsets are all correlated with NHML surface aerosol forcing ( $r = 0.57$ ,  $r = 0.64$  and  $r = 0.51$  respectively,  $P < 0.05$ ). The land precipitation offset–aerosol forcing correlation is largely independent of the observed precipitation data set chosen, which provide temporally varying spatial masks for the model-simulated output (Supplementary Fig. 4).

Using the temperature gradient offset–aerosol forcing regression coefficients, the observed temperature offset of  $-0.36 \pm 0.14$  K (5–95% uncertainty range) corresponds to an aerosol forcing of  $-3.5 \pm 1.2$  W m<sup>-2</sup>, compared with an IPCC equivalent NHML surface aerosol forcing of  $-2.0$  ( $-3.3$  to  $-0.9$ ) W m<sup>-2</sup> (Supplementary Note and Fig. 5). The difference is a consequence of the likely ocean circulation-driven abrupt decrease in the observed mean temperature gradient in the late 1960s (ref. 17). Removing this abrupt shift (Supplementary Note) and assuming the CMIP5 models fail to simulate such internal variability<sup>16</sup>, a corrected temperature offset more indicative of a response to just anthropogenic aerosol forcing of  $-0.15 \pm 0.04$  K gives an aerosol forcing of  $-1.7 \pm 0.4$  W m<sup>-2</sup>. The observed NHT land precipitation offset agrees well with the IPCC equivalent NHML surface aerosol forcing. Here, the offset of  $-0.065 \pm 0.062$  mm d<sup>-1</sup> gives an aerosol forcing of  $-1.7 \pm 1.8$  W m<sup>-2</sup>.

The observed NHML land precipitation offset of  $+0.025 \pm 0.016$  mm d<sup>-1</sup> seems to contradict both the observed temperature gradient offset and the observed NHT land precipitation offset, while equivalent to an aerosol forcing of  $+1.5 \pm 1.6$  W m<sup>-2</sup>, calculated using the NHML land precipitation offset–aerosol forcing regression coefficients. This is clearly inconsistent with the IPCC equivalent NHML surface aerosol forcing. This could imply that the correlation across CMIP5 models is not robust. We note, however, that the observed NHML land precipitation offset is likely to be more positive than all but two models masked to the GHCN data set when considering the four observed data sets (Fig. 3c and Supplementary Fig. 4). Also, we find a considerably

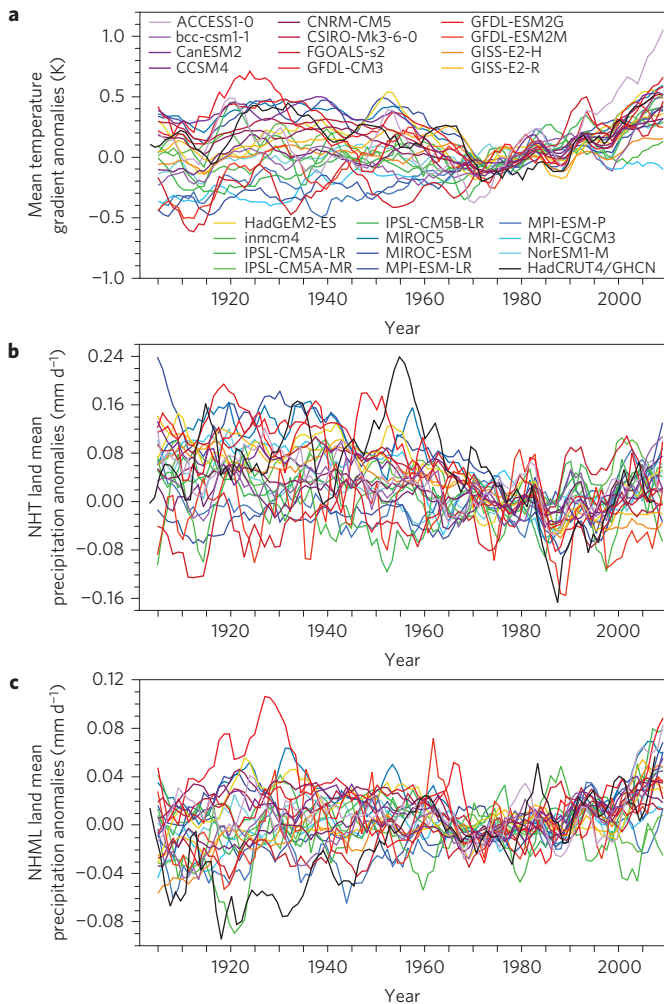


**Figure 2 | Time series of mean temperature and precipitation for 1905–2004. a**, Mean temperature gradient anomalies. **b**, Northern Hemisphere tropical (NHT) land mean precipitation anomalies. **c**, Northern Hemisphere mid-latitude (NHML) land mean precipitation anomalies. Model data (coloured lines) are from 23 CMIP5 models (Supplementary Table 1) and observed data (black lines) are from the HadCRUT4 and GHCN data sets for temperature and precipitation respectively (Methods). All model data are masked to the observations and anomalized with respect to the period 1961–1990 (Methods).

stronger correlation with the removal of the GISS-E2-H and GISS-E2-R climate models ( $r = 0.65$ ,  $P < 0.01$ ), which have anomalously strong NHML surface long-wave forcing (Supplementary Fig. 6), thus nullifying the response to aerosol forcing.

If the latest climate models do adequately simulate twentieth-century land precipitation response to aerosol<sup>20,21</sup>, an intriguing possibility is that trends in observed NHML land precipitation are unreliable. Significant precipitation gauge measurement biases have been previously identified, particularly in high-latitude regions<sup>10</sup>. Efforts to correct observations from recent decades for biases have resulted in increases in global land mean precipitation totals of 11.7% (ref. 22) and increases in winter higher mid-latitudes precipitation totals of 20–40% (ref. 23). For century-scale observations time series inhomogeneities due to changes in instrumentation and recording practices can bias the true precipitation variability<sup>24</sup> and even change the sign of precipitation trends in some regions<sup>25</sup>.

One region where numerous measurement errors have been documented is the former Soviet Union. For example, in 1966 a

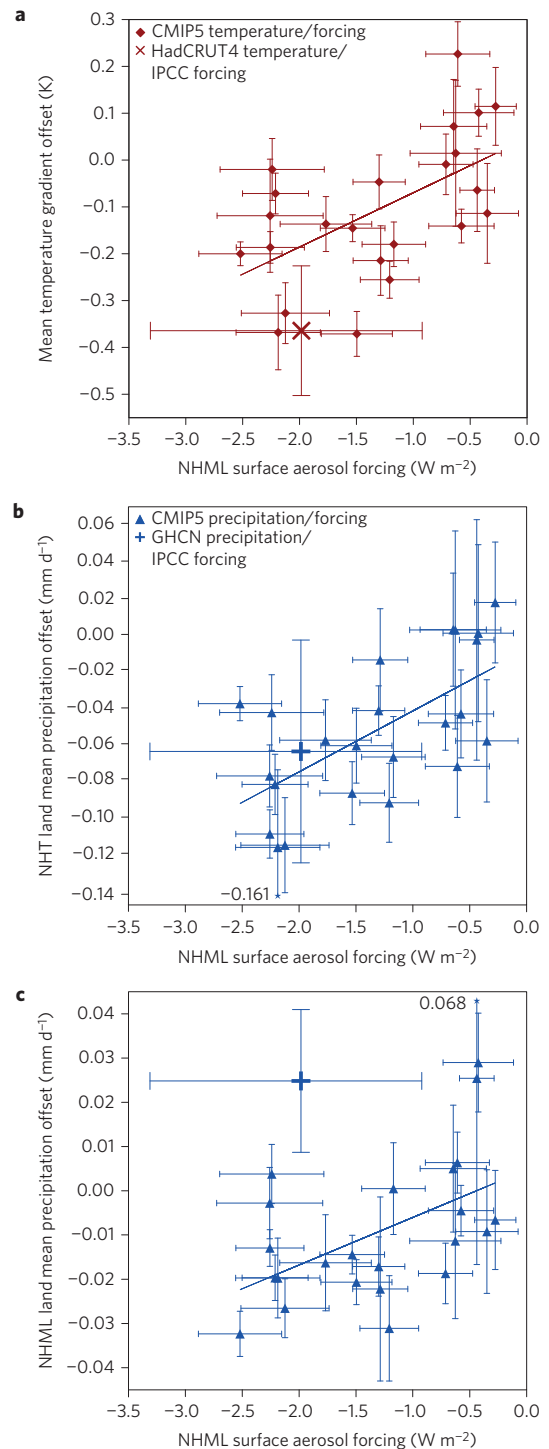


**Figure 3 | Comparing temperature gradient and precipitation offsets with the strength of Northern Hemisphere mid-latitude (NHML) surface aerosol forcing. a**, Mean temperature gradient offset against NHML surface aerosol forcing. **b**, Northern Hemisphere tropical (NHT) land mean precipitation offset against NHML surface aerosol forcing. **c**, NHML land mean precipitation offset against NHML surface aerosol forcing. Error bars represent the 5–95% uncertainty range (Methods), with IPCC equivalent NHML surface aerosol forcing and the associated 5–95% uncertainty range used for the observed data points (Supplementary Note and Fig. 5). The proximity of the observed data points to the regression lines can be seen as indicative of the level of agreement between observations and models. The values next to the error bars in **b** and **c** indicate where the uncertainties extend beyond the scale.



wetting correction was introduced that increased typical individual station annual totals by 5–15% and in extreme cases by up to 30% for more northerly stations in winter<sup>9,10</sup>. However, even correcting each individual station in the former Soviet Union before inclusion in a gridded data set would require extensive study of metadata, which may not exist<sup>9</sup>, meaning that conventional NHML bias correction may not be possible. An alternative is to explore possible biases in the Climatic Research Unit (CRU) and Global Precipitation Climatology Centre (GPCC) data sets using our physical framework that links aerosol, temperature and precipitation change (Methods). An increase of 2.9% and 2.4% in monthly total precipitation before 1960 for CRU and GPCC respectively would generate NHML land precipitation offsets consistent with estimated aerosol forcing, the temperature gradient offset and the NHT land precipitation offset (Supplementary Fig. 7). Although this approach is crude, it serves to illustrate how sensitive trends in precipitation are to inhomogeneities of a magnitude frequently found in studies.

The effect of aerosols on regional temperature has been shown previously<sup>1,2</sup>. We find a detectable mean temperature gradient response to aerosol forcing, the size of which is dependent on the strength of aerosol forcing. Using this relationship, observed temperature is found to be in keeping with the estimated strength of real-world aerosol forcing. In agreement with existing literature, the NHT land mean precipitation response to remote extratropical aerosol forcing is found to be predictable across models, with observations again fitting into this framework. Theory suggests that aerosols should also have a significant impact on NHML land mean precipitation. Again, this is the case in CMIP5 models with stronger aerosol forcing correlated with a larger negative precipitation response. However, the observed NHML land mean precipitation response suggests that twentieth-century NHML aerosol forcing was positive, in disagreement with the modelled response and the scientific consensus on aerosol radiative effects.

The NHML region should contain our most valuable century-long observations. It is possible that model simulations of NHML land mean precipitation response to aerosol forcing are incorrect. Perhaps land surface processes such as soil moisture availability<sup>26</sup> are of large importance and are misrepresented by present models. However, there is evidence that present widely used precipitation data sets may still contain significant biases, particularly in the early twentieth century, which restricts many precipitation studies to the second half of the twentieth century. It may be that, despite poorer spatial and temporal coverage, NHT land precipitation observations are more reliable through avoidance of measurement difficulties associated with high-latitude climate, such as snowfall undercatch. With scientific conclusions often based on agreement with observed data sets that are taken as truth<sup>9</sup> it is imperative that inhomogeneities in existing precipitation records are considered further. The NHML region is one of the most densely populated regions of the world. An improved understanding of past precipitation would help towards improved regional-scale projections of the future, which are of huge value to policymakers.

## Methods

**Regridding and masking.** The NHML region is defined as the latitude band bounded by 30° N and 65° N. However, the findings are largely insensitive to slight shifts in these bounds, with NHML storm tracks always captured. The SHEXT region is the latitude band bounded by 30° S and 90° S. We use three other gridded observational precipitation data sets, in addition to the GHCN data set that is used in the main analyses. These are an updated version of the Zhang data set<sup>21</sup>, the latest CRU high-resolution precipitation data set<sup>27</sup> and the GPCC Full Data Reanalysis V6 data set<sup>28</sup>. The CRU and GPCC data sets are spatially interpolated, but here we consider only grid boxes where real observations exist. These data (CRU and GPCC) are gridded to the same 5° × 5° grid and anomalized with respect to the period 1961–1990 (the years with most available observations) to be consistent with the GHCN and Zhang data sets, as well as the HadCRUT4 temperature observations. However, for the correction analysis

(Supplementary Fig. 7) we use CRU and GPCC monthly total precipitation values. The four precipitation data sets are not masked to be spatially and temporally consistent with each other. Different data sets contain different station records, with some favouring fewer long-term homogenized records and others selecting a much greater number of short-term records, thus testing the sensitivity of the analyses to varying spatial and temporal coverage<sup>29</sup>. For the HadCRUT4 gridded global surface temperature anomalies data set we use the median of the 100 ensemble members available. All model data are first regridded to the common 5° × 5° grid. For simulated precipitation, we mask to each of the four observed data sets in turn, apart from in Fig. 1a, where unmasked global means are shown. Simulated temperature is masked to the HadCRUT4 data set (land and ocean) in all instances. Following masking, data are anomalized relative to the 1961–1990 period, apart from in Fig. 1, where data are anomalized with respect to the mean of a pre-industrial control simulation.

**Forcing.** Forcing time series are calculated using a simple linear forcing–feedback model<sup>30</sup>, although we consider only short-wave radiative fluxes. Surface forcing is calculated by looking at just surface fluxes. Model simulated radiative fluxes are regridded to the common 5° × 5° grid. The strength of NHML surface aerosol forcing in models is diagnosed by taking the difference between mean NHML mean surface short-wave forcing before and after 1960. NHML surface short-wave forcing from a historical all-forcings experiment is largely representative of NHML surface total forcing from a historical anthropogenic aerosol forcings alone experiment (Supplementary Fig. 8), particularly when considering the difference between two long-term means. Surface aerosol forcing is used, because both increasing black carbon aerosol and increasing sulphate aerosol atmospheric concentrations lead to negative surface aerosol forcing and—albeit through different mechanisms—are expected to generate a negative precipitation offset in the mid twentieth century<sup>14</sup>. Horizontal error bars for CMIP5 models in Fig. 3 and Supplementary Figs 4 and 6 show an estimate of the 5–95% uncertainty ranges in NHML surface aerosol forcing. Calculation of NHML surface aerosol forcing error bars for observations follows the method outlined in the Supplementary Note and Fig. 5.

**Calculating the precipitation/temperature offsets.** To calculate, for example, the size of the NHML land mean precipitation offset,  $\beta$ , we consider the precipitation–temperature relationship (Fig. 1c) and fit a simple linear regression model to the data

$$\beta \mathbf{1} = \mathbf{P}_{60-04} - \overline{P_{05-59}} \mathbf{1} - \gamma (\mathbf{T}_{60-04} - \overline{T_{05-59}} \mathbf{1})$$

where  $\mathbf{1}$  is a column vector of all ones,  $\overline{P_{05-59}}$  represents the mean NHML land mean precipitation anomaly for 1905–1959,  $\mathbf{P}_{60-04}$  represents five-year mean NHML land mean precipitation anomalies for 1960–2004,  $\overline{T_{05-59}}$  represents the mean global mean temperature anomaly for 1905–1959,  $\mathbf{T}_{60-04}$  represents five-year mean global mean temperature anomalies for 1960–2004 and  $\gamma$  is the trend from the linear regression fit to 1960–2004 NHML land mean precipitation–global mean temperature. Vertical error bars for CMIP5 models in Fig. 3 and Supplementary Fig. 4 show an estimate of the 5–95% uncertainty ranges in  $\beta$ . This regression model is fitted to each model separately, as well as the observations. An identical technique is implemented to measure the NHT land mean precipitation offsets and temperature gradient offsets.

Received 28 October 2013; accepted 24 February 2014;  
published online 30 March 2014

## References

- Stott, P. Attribution of regional-scale temperature changes to anthropogenic and natural causes. *Geophys. Res. Lett.* **30**, 1728–1731 (2003).
- Shindell, D. & Faluvegi, G. Climate response to regional radiative forcing during the twentieth century. *Nature Geosci.* **2**, 294–300 (2009).
- Shindell, D. T., Voulgarakis, A., Faluvegi, G. & Milly, G. Precipitation response to regional radiative forcing. *Atmos. Chem. Phys.* **12**, 6969–6982 (2012).
- Allen, M. R. & Ingram, W. J. Constraints on future changes in climate and the hydrologic cycle. *Nature* **419**, 224–232 (2002).
- Lambert, F. H. & Allen, M. R. Are changes in global precipitation constrained by the tropospheric energy budget? *J. Clim.* **22**, 499–517 (2009).
- Chang, C.-Y., Chiang, J. C. H., Wehner, M. F., Friedman, A. R. & Ruedy, R. Sulfate aerosol control of tropical Atlantic climate over the twentieth century. *J. Clim.* **24**, 2540–2555 (2011).
- Hwang, Y.-T., Frierson, D. M. W. & Kang, S. M. Anthropogenic sulphate aerosol and the southward shift of tropical precipitation in the late 20th century. *Geophys. Res. Lett.* **40**, 2845–2850 (2013).
- Myhre, G. *et al.* in *Climate Change 2013: The Physical Science Basis* (eds Stocker, T. F. *et al.*) Ch. 8. (Cambridge Univ. Press, 2013).

9. Groisman, P. Y. & Rankova, E. Y. Precipitation trends over the Russian permafrost-free zone: Removing the artifacts of pre-processing. *Int. J. Climatol.* **21**, 657–678 (2001).
10. Groisman, P. Y., Koknaeva, V. V., Belokrylova, T. A. & Karl, T. R. Overcoming biases of precipitation measurement: A history of the USSR experience. *Bull. Am. Meteorol. Soc.* **72**, 1725–1733 (1991).
11. Hegerl, G. C. *et al.* in *IPCC Climate Change 2007: The Physical Science Basis* (eds Solomon, S. *et al.*) Ch. 10. (Cambridge Univ. Press, 2007).
12. Lamarque, J. F. *et al.* Historical (1850–2000) gridded anthropogenic and biomass burning emissions of reactive gases and aerosols: Methodology and application. *Atmos. Chem. Phys.* **10**, 7017–7039 (2010).
13. Lambert, F. H. & Faull, N. E. Tropospheric adjustment: The response of two general circulation models to a change in insolation. *Geophys. Res. Lett.* **34**, L03701 (2007).
14. Andrews, T. *et al.* Precipitation, radiative forcing and global temperature change. *Geophys. Res. Lett.* **37**, L14701 (2010).
15. Morice, C. P., Kennedy, J. J., Rayner, N. A. & Jones, P. D. Quantifying uncertainties in global and regional temperature change using an ensemble of observational estimates: The HadCRUT4 data set. *J. Geophys. Res.* **117**, D08101 (2012).
16. Friedman, A. R., Hwang, Y.-T., Chiang, J. C. H. & Frierson, D. M. W. Interhemispheric temperature asymmetry over the twentieth century and in future projections. *J. Clim.* **26**, 5419–5433 (2013).
17. Thompson, D. W. J., Wallace, J. M., Kennedy, J. J. & Jones, P. D. An abrupt drop in Northern Hemisphere sea surface temperature around 1970. *Nature* **467**, 444–447 (2010).
18. Vose, R. S. *et al.* *The Global Historical Climatology Network: Long-Term Monthly Temperature, Precipitation, Sea Level Pressure, and Station Pressure Data*. Report ORNL/CDIAC-53, NDP-041 (Carbon Dioxide Information Analysis Center, Oak Ridge National Laboratory, 1992); <http://cdiac.esd.ornl.gov/ftp/ndp041/ndp041.pdf>
19. Wild, M. Enlightening global dimming and brightening. *Bull. Am. Meteorol. Soc.* **93**, 27–37 (2012).
20. Wu, P., Christidis, N. & Stott, P. Anthropogenic impact on Earth's hydrological cycle. *Nature Clim. Change* **3**, 807–810 (2013).
21. Zhang, X. *et al.* Detection of human influence on twentieth-century precipitation trends. *Nature* **448**, 461–465 (2007).
22. Adam, J. C. & Lettenmaier, D. P. Adjustment of global gridded precipitation for systematic bias. *J. Geophys. Res.* **108**, 4257 (2003).
23. Yang, D., Kane, D., Zhang, Z., Legates, D. & Goodison, B. Bias corrections of long-term (1973–2004) daily precipitation data over the northern regions. *Geophys. Res. Lett.* **32**, L19501 (2005).
24. Legates, D. R. Global and terrestrial precipitation: A comparative assessment of existing climatologies. *Int. J. Climatol.* **15**, 237–258 (1995).
25. Ding, Y., Yang, D., Ye, B. & Wang, N. Effects of bias correction on precipitation trend over China. *J. Geophys. Res.* **112**, D13116 (2007).
26. Koster, R. D. *et al.* Regions of strong coupling between soil moisture and precipitation. *Science* **305**, 1138–1140 (2004).
27. Harris, I., Jones, P. D., Osborn, T. J. & Lister, D. H. Updated high-resolution grids of monthly climate observations—the CRU TS3.10 dataset. *Int. J. Climatol.* **34**, 623–642 (2013).
28. Becker, A. *et al.* A description of the global land-surface precipitation data products of the Global Precipitation Climatology Centre with sample applications including centennial (trend) analysis from 1901–present. *Earth Syst. Sci. Data* **5**, 71–99 (2013).
29. Beck, C., Grieser, J. & Rudolf, B. *A New Monthly Precipitation Climatology for the Global Land Areas for the Period 1951–2000*. *Climate Status Report 2004* (German Weather Service, 2005).
30. Forster, P. M. *et al.* Evaluating adjusted forcing and model spread for historical and future scenarios in the CMIP5 generation of climate models. *J. Geophys. Res.* **118**, 1139–1150 (2013).

### Acknowledgements

We acknowledge the World Climate Research Programme's Working Group on Coupled Modelling, which is responsible for CMIP, and we thank the climate modelling groups (listed in Supplementary Table 1 of this paper) for producing and making available their model output. For CMIP the US Department of Energy's Program for Climate Model Diagnosis and Intercomparison provides coordinating support and led development of software infrastructure in partnership with the Global Organization for Earth System Science Portals. We thank X. Zhang for provision of the Zhang data set and for useful discussions. We also thank C. Ferro for helpful insight. J.M.O. is supported by an EPSRC studentship.

### Author contributions

Both authors designed the study, discussed results and revised the manuscript. J.M.O. performed the analysis and wrote the manuscript.

### Additional information

Supplementary information is available in the [online version of the paper](#). Reprints and permissions information is available online at [www.nature.com/reprints](http://www.nature.com/reprints). Correspondence and requests for materials should be addressed to J.M.O.

### Competing financial interests

The authors declare no competing financial interests.